# Method of Identifying Dynamic Multileaf Collimator Irradiation that is Highly Sensitive to a Systematic MLC Calibration Error

P. Zygmanski, J. H. Kung

Department of Radiation Oncology, Massachusetts General Hospital and Harvard Medical School
Boston, MA
*E-mail: jkung@partners.org*

## ABSTRACT

In Intensity Modulated Radiotherapy (IMRT), radiation is delivered in a multiple of Multileaf Collimator (MLC) subfields. A subfield with a small leaf-to-leaf opening is highly sensitive to a leaf-positional error. We introduce a method of identifying and rejecting IMRT plans that are highly sensitive to a systematic MLC gap error (sensitivity to possible random leaf-positional errors is not addressed here). There are two sources of a systematic MLC gap error: Centerline Mechanical Offset (CMO) and, in the case of a rounded end MLC, Radiation Field Offset (RFO). In IMRT planning system, using an incorrect value of RFO introduces a systematic error ΔRFO that results in all leaf-to-leaf gaps that are either too large or too small by (2 · ΔRFO), whereas assuming that CMO is zero introduces systematic error ΔCMO that results in all gaps that are too large by ΔCMO = CMO.

We introduce a concept of the Average Leaf Pair Opening (ALPO) that can be calculated from a dynamic MLC delivery file. We derive an analytic formula for a fractional average fluence error resulting from a systematic gap error of $\Delta x$ and show that it is inversely proportional to ALPO; explicitly it is equal to $\frac{\Delta x}{ALPO + 2 \cdot RFO + \varepsilon}$, in which $\varepsilon$ is generally of the order of 1 mm and Δx=2·ΔRFO+CMO. This analytic relationship is verified with independent numerical calculations.

**Key Words**: Intensity Modulated Radiotherapy, Multileaf Collimator, Quality Assurance

## 1. INTRODUCTION

In Intensity Modulated Radiotherapy (IMRT), radiation is delivered in a multiple of Multileaf Collimator (MLC) subfields[1-6]. Subfields with a small leaf-to-leaf opening are highly sensitive to a MLC leaf-positional error[7-9]. LoSasso[8] noted that for a 1 cm sweeping window dynamic MLC delivery, a systematic 1 mm leaf-to-leaf gap error to all leaf pairs will result in about 10% fluence error. Further, Chui et al.[7] have proposed several film and ion chamber tests to ensure a 1mm precision in leaf positions.

There are two sources of a systematic MLC gap error $\Delta x$: neglecting Centerline Mechanical Offset (CMO)[10], and imprecise determination of Radiation Field Offset (RFO) in the case of a rounded end MLC[8,11-14]. By a systematic error, we mean an error of constant value to all leaves at every leaf position. Random leaf-positional errors are not addressed in our analysis. CMO is used to prevent leaf-to-leaf collision at zero gap opening. For example for CMO = 0.5 mm and digital leaf-to-leaf separation encoded at 1 cm, the true light field size at Source to Axial Distance (SAD) will be 1.05 cm[10]. RFO is used by a treatment planning system to compensate for the penetration of radiation into rounded leaf ends, e.g., with RFO = 1 mm, to create a radiation field of 1 cm at SAD, leaves must receive instruction to create a geometrical field of (10-2·1) mm = 8 mm at SAD[8,11-14].

In IMRT planning system, using an incorrect value of RFO introduces a systematic error ΔRFO that results in all leaf-to-leaf gaps that are either too large or too small by (2 · ΔRFO), whereas assuming that CMO is zero introduces systematic error ΔCMO that results in all gaps that are too large by ΔCMO = CMO. Thus the total systematic error becomes Δx= 2 · ΔRFO + CMO. A new feature of calibrating an MLC for its use in IMRT is to determine the beam energy dependent RFO value, and to verify that dosimetry for IMRT plans is accurate for the RFO and non-zero CMO values that are used. For a brief outline of the MLC calibration procedure the reader is referred to Klein [10]. Kung and Chen[15] have studied dose perturbations in IMRT plans resulting from these systematic gap errors. The magnitude of dose perturbation to a target volume per mm of a systematic gap error was found to vary from one IMRT plan to another; they introduced a method of calculating Equivalent Monitor Unit Error (EMUE) resulting from a dynamic MLC delivery with a systematic gap error. The EMUE was used to estimate dose error to a target volume and to

identify and reject IMRT plans (e.g., dynamic MLC delivery) that were highly sensitive to a systematic gap error. In this technical note, we introduce a simpler concept of an Average Leaf Pair Opening (ALPO) as a counterpart to the EMUE calculation. The utility of ALPO is as follows. A value of ALPO can be calculated from a dynamic MLC file of an IMRT plan. We prove that fractional average fluence error from a systematic gap error of $\Delta x$ is $\Delta x/(ALPO + 2 \cdot RFO + \varepsilon)$, where $\varepsilon$ is of the order of 1 mm. As an example, for $\Delta x = 1$ mm, ALPO = 1 cm, RFO = 1 mm, $\varepsilon = 1$ mm fluence error is 6 %.

Several authors have quoted different values of RFO for 6 MV Varian rounded end MLC, i.e., $\mathrm{RFO} = (0.2 - 0.95)$ mm[8,11-14]. With the concept of ALPO, we address the problem of discrepancies in quoted values of RFO by different institutions. Further we answer the question of what would be a dosimetric consequence of switching from one RFO value to another. We propose that ALPO can be used to identify and to reject a dynamic MLC delivery that is highly sensitive to a systematic MLC gap error.

The layout of the technical note is as follows. The concept of ALPO is introduced in Sec. II A. Numerical and analytical methods of calculating a fractional fluence error from a systematic gap error of $\Delta x$ are explained in Sec. II B & C and Sec. II D, respectively. The numerical simulation results are used as benchmark values to verify the analytic relationship between a fractional fluence error and ALPO. In Sec. II E & F, we describe two tests comparing the analytic and numerical calculations; the results are given in Sec. III A& B. In this note, we use the term dynamic MLC to mean both step & shoot and sliding window delivery techniques.

## 2. MATERIALS AND METHODS

### 2.1. The concept of Average Leaf Pair Opening (ALPO)

Let us consider a dynamic MLC file of an IMRT plan. We define a quantity of Average Leaf Pair Openings (ALPO) of a dynamic MLC as

$$ALPO = \frac{\sum_{s,j} |x_R - x_L|_{s,j} \Delta MU_s}{\sum_{s,j=\text{open pairs}} \Delta MU_s} \qquad (1)$$

where s= MLC subfield index, j = leaf pair index, $\Delta MU_s$ = Monitor Units delivered in the subfield (s), $X_R(X_L)$ = right (left) leaf positions at SAD in Beam's Eye View (BEV).

In Eq. (1), the sum is over all subfields (s) and over all leaf pairs with a non-zero leaf-to-leaf opening. As an example, consider a limiting case of a step and shoot dynamic MLC delivery that has only one segment delivered with 2MU (Fig. 1(a)). Then from Eq. (1),

$$ALPO = \frac{(2cm \cdot 2MU + 5cm \cdot 2MU + 2cm \cdot 2MU)}{2MU + 2MU + 2MU} = 3\ cm \qquad (2)$$

A slightly more realistic example is a step and shoot dynamic MLC delivery with two segments of 2 MU and 6 MU (Fig. 1(a) & 1(b)). Here ALPO is

$$ALPO = \frac{(2 \cdot 2 + 5 \cdot 2 + 2 \cdot 2)cm \cdot MU + (1 \cdot 6 + 3 \cdot 6 + 1 \cdot 6)cm \cdot MU}{(2 + 2 + 2)MU + (6 + 6 + 6)MU} = 2\ cm \qquad (3)$$

The definition of ALPO in Eq. (1) uses geometrical leaf positions taken from a dynamic MLC file. As mentioned in the introduction, for a rounded-end MLC effective radiation field sizes along the leaf-to-leaf direction are larger than the corresponding geometrical sizes at SAD by $2 \cdot RFO$. We could have as well introduced a concept of Average Leaf Pair Opening using radiation field sizes, which would have differed from Eq. (1) by $2 \cdot RFO$.

For a sliding window dynamic MLC delivery, in which leaves move while radiation is on, the discrete sum in Eq. (1) can be evaluated if a continuous leaf motion is approximated by multiple of static leaf positions. An exact and numerically simpler method of evaluating sum in Eq. (1) for a sliding window dynamic MLC can be understood with the aid of Figure 1(c), which shows trajectories of a single leaf pair. The numerator of Eq. (1) is then recognized as a sum of "area" generated by leaf pair trajectories in the phase space of leaf coordinates and monitor units (x-MU space). The denominator is recognized as a sum of fractional MU during which a leaf pair was open.

We wrote programs in Interactive Data Language (IDL), (RSI Inc) to calculate ALPO. The input to the program are the leaf positions from a dynamic (sliding window) MLC file (Varian format) of an IMRT plan.

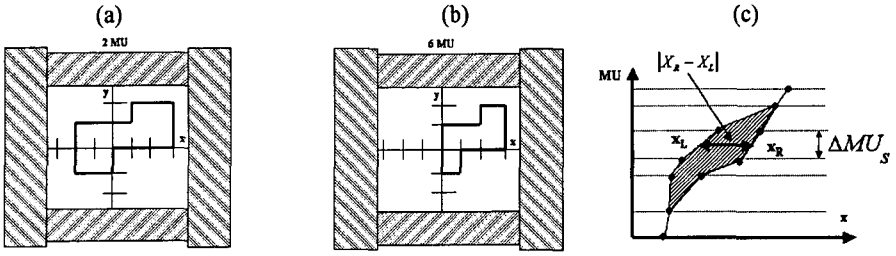


Figure 1. (a) A dynamic MLC subfield delivered with 2 MU. (b) A dynamic MLC subfield delivered with 6 MU. (c) An example of a sliding window dynamic MLC trajectories for a leaf pair.

### 2.2. Definition and numerical calculation of average fluence $\langle\Phi\rangle_{\sigma(PTV)}$

Let $\Phi(x,y)$ denote a fluence in Monitor Units (Fig. 2a) in air; x and y are coordinates in BEV. For step and shoot dynamic MLC, $\Phi(x,y)$ can be numerically calculated by ray tracing and Monitor Units projecting method[16]. We will restrict ourselves to the Varian type of dynamic MLC in which jaws are fixed during leaf motions, e.g., collimator scatter factor is constant. For each static subfield, we ray trace each subfield's aperture area and project the MU of a corresponding subfield onto a grid. For regions inside the jaws but blocked by the MLC, we include 1.5% of MU of the subfield as a transmission fluence. In the ray tracing, because of the RFO, all radiation field sizes along the leaf end direction are larger than the corresponding digital leaf positions of dynamic MLC by the value of RFO.

An average fluence over BEV's planning target volume's (PTV) cross sectional area $\sigma(PTV)$ is

$$\langle\Phi\rangle_{\sigma(PTV)} \equiv \frac{\int_{\sigma(PTV)}\Phi(x,y)dxdy}{\int_{\sigma(PTV)}dxdy} \tag{4}$$

For a sliding window dynamic MLC delivery, the above method can again be made to work without any change if continuous leaf motions are approximated by a multiple of static leaf positions. However, as stated before, there exists an alternate and numerically simpler method, which is equivalent to ray tracing and projection method. This alternate method can be understood with the aid of Figure 2(b). At each point of $\Phi(x,y)$ grid, we calculate fractional Monitor Units for which a leaf pair was opened at (x,y). The contribution from a transmission fluence is again calculated as 1.5% of fractional Monitor Units for which a leaf pair was closed at (x,y). As in the case of step and shoot dynamic MLC, the effect of RFO is to make all radiation field sizes larger than the corresponding light field sizes by 2·RFO. For a sliding window dynamic MLC, a leaf opening can take almost any value from several cm to zero cm. Therefore, we arbitrarily used a criterion of 1 mm in deciding whether a leaf pair was opened or closed, and only to those open leaf pairs were radiation fields sizes made larger than the corresponding light fields by 2·RFO.

### 2.3. Definition and numerical calculation of fractional fluence error $\frac{\langle\delta\Phi_{\Delta x}\rangle_{\sigma(PTV)}}{\langle\Phi\rangle_{\sigma(PTV)}}$

If there is a systematic MLC gap error of $\Delta x$, either from using a non-zero CMO or inaccurate RFO value, then there will be an error to leaf coordinates, i.e.,

$$\begin{aligned} x_R &= x_R + \Delta x/2 \\ x_L &= x_L - \Delta x/2 \end{aligned} \tag{5}$$

$\Delta x = \mathrm{CMO} + 2\cdot\Delta\mathrm{RFO}$, where $\Delta\mathrm{RFO}$ is an error in RFO value used in a treatment planning system. In Eq. (5), we have assumed that the gap error is symmetric for both right and left leaves, but as it will become clear this assumption does not effect the calculation of average fluence error.

Let $\Phi_{\Delta x}(x,y)$ denote a composite fluence in air if there is a systematic gap error of $\Delta x$. The numerical calculation of $\Phi_{\Delta x}(x,y)$ is identical to calculation of $\Phi(x,y)$ except that in ray tracing leaf position, besides the RFO offset, there is an additional offset given by Eq. (5). Then

$$\left\langle \Phi_{\Delta x} \right\rangle_{\sigma(PTV)} \equiv \frac{\int_{\sigma(PTV)} \Phi_{\Delta x}(x,y)dxdy}{\int_{\sigma(PTV)} dxdy} \tag{6}$$

We define an average fluence error $\left\langle \delta\Phi_{\Delta x} \right\rangle_{\sigma(PTV)}$ in air from a systematic gap error of $\Delta x$ by

$$\left\langle \delta\Phi_{\Delta x} \right\rangle_{\sigma(PTV)} \equiv \left\langle \Phi_{\Delta x} \right\rangle_{\sigma(PTV)} - \left\langle \Phi \right\rangle_{\sigma(PTV)} \tag{7}$$

A fractional average fluence error in air, for an individual IMRT field, can be calculated by $\frac{\left\langle \delta\Phi_{\Delta x} \right\rangle_{\sigma(PTV)}}{\left\langle \Phi \right\rangle_{\sigma(PTV)}}$.

We wrote programs in IDL to numerically calculate $\frac{\left\langle \delta\Phi_{\Delta x} \right\rangle_{\sigma(PTV)}}{\left\langle \Phi \right\rangle_{\sigma(PTV)}}$. The input to the program is the leaf positions from a dynamic (sliding window) MLC file of an IMRT plan. We used MLC transmission T=1.5%, and RFO = 0.75 mm for a 6 MV Varian 26 leaf pair MLC.

The fluence $\Phi(x,y)$ grid size was 1 mm along the direction of leaf motion direction and 1 cm for the leaf width. For the numerical study, we used $\Delta x = 1$ mm. For a step and shoot dynamic MLC, the effect of a gap error is to concentrate fluence errors only along leaf end positions, which are static. Therefore, the grid size along the leaf motion direction must be finer than the dimension of gap error $\Delta x$ under investigation. This restriction does not apply if a numerical calculation of $\Phi(x,y)$ for sliding widow dynamic MLC is calculated with the method illustrated in (Fig. 2(b)). This is because for a sliding window dynamic MLC, a change in gap essentially changes only the length of time over which a leaf pair is opened at (x, y).

(a) (b)

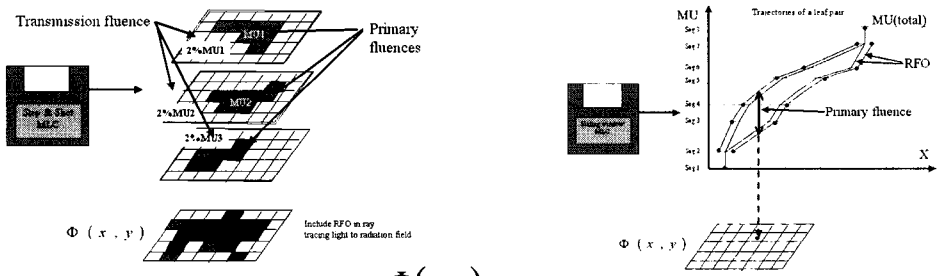


Figure 2. (a) A schematic of numerical calculation of $\Phi(x,y)$ from a step and shoot dynamic MLC file. (b) A schematic of numerical method of calculating $\Phi(x,y)$ for a sliding window dynamic MLC file.

### 2.4. Analytic calculation of fractional average fluence error $\frac{\left\langle \delta\Phi_{\Delta x} \right\rangle_{\sigma(PTV)}}{\left\langle \Phi \right\rangle_{\sigma(PTV)}}$ and its relations to ALPO and $\Delta x$

We would like to evaluate the expression for $\left\langle \Phi \right\rangle_{\sigma(PTV)}$ (Eq. 4) analytically. We will give the derivation for step and shot dynamic MLC, but the result is also valid for sliding window dynamic MLC. The derivation will be in three steps with each step of increasing complexity.

*(i)* T = 0, RFO = 0

Let us first consider a simpler case of zero MLC transmission (i.e., T = 0) and RFO = 0. Notice from Fig. 2(a), $\left\langle \Phi \right\rangle_{\sigma(PTV)}$ can be written as

$$\left\langle \Phi^{T=0,RFO=0} \right\rangle_{\sigma(PTV)} = \frac{\int_{\sigma(PTV)} \Phi^{T=0,RFO=0}(x,y)dxdy}{\sigma(PTV)} = \frac{\sum_s \Delta MU_s \cdot A_s}{\sigma(PTV)} = \frac{\sum_{s,j} |x_R - x_L|_{s,j} \, \Delta MU_s \cdot w}{\sigma(PTV)} \tag{8}$$

where $A_s$, is area of MLC subfield with index (s), and $\Delta MU_s$ is the number of monitor units delivered in MLC subfield (s). We have substituted $A_s = \sum_j |x_R - x_L|_{s,j} \; w$, where $|x_R - x_L|_{s,j}$ is the leaf-to-leaf opening at SAD for leaf pair (j) in subfield (s), and $w$ is the width leaf at SAD (e.g., 1 cm leaf width).
Eq. ( 8) allows for analytic development. Now, if there is a systematic MLC gap error of $\Delta x$, then by Eq. (5),

$$\left\langle \Phi_{\Delta x}{}^{T=0,RFO=0} \right\rangle_{\sigma(PTV)} = \frac{\sum_{s,j} |x_R - x_L + \Delta x|_{s,j} \; \Delta MU_s \cdot w}{\sigma(PTV)} = \left\langle \Phi^{T=0,RFO=0} \right\rangle_{\sigma(PTV)} + \frac{w \cdot \Delta x}{\sigma(PTV)} \sum_{s,j=\text{openpair}} \Delta MU_s \tag{9}$$

And therefore from definition of ALPO Eqs. (1) and (7),

$$\frac{\left\langle \delta\Phi_{\Delta x}^{T=0,RFO=0} \right\rangle_{\sigma(PTV)}}{\left\langle \Phi^{T=0,RFO=0} \right\rangle_{\sigma(PTV)}} = \frac{\left\langle \Phi_{\Delta x}^{T=0,RFO=0} \right\rangle_{\sigma(PTV)} - \left\langle \Phi^{T=0,RFO=0} \right\rangle_{\sigma(PTV)}}{\left\langle \Phi^{T=0,RFO=0} \right\rangle_{\sigma(PTV)}} = \Delta x \cdot \frac{\sum_{s,j=\text{open pairs}} \Delta MU_s}{\sum_{s,j} |x_R - x_L|_{s,j} \Delta MU_s} = \frac{\Delta x}{ALPO} \tag{10}$$

*(ii)* $\mathrm{T} = 0, \; \mathrm{RFO} \neq 0$

Now, let us include the effect from RFO. With a non-zero RFO value for a rounded end MLC, all radiation field sizes along leaf end directions are larger by $2 \cdot RFO$, i.e.,

$$|x_R - x_L|_{s,j} \rightarrow |x_R - x_L|_{s,j} + 2 \cdot \mathrm{RFO} \tag{11}$$

Therefore,

$$\left\langle \Phi^{T=0} \right\rangle_{\sigma(PTV)} = \frac{\sum_{s,j} |x_R - x_L|_{s,j} \; \Delta MU_s w}{\sigma(PTV)} + \frac{2 \cdot RFO \cdot w}{\sigma(PTV)} \sum_{s,\, j=\text{openpair}} \Delta MU_s \tag{12a}$$

$$\left\langle \Phi_{\Delta X}{}^{T=0} \right\rangle_{\sigma(PTV)} = \left\langle \Phi^{T=0} \right\rangle_{\sigma(PTV)} + \frac{w \cdot \Delta x}{\sigma(PTV)} \sum_{s,\, j=\text{openpair}} \Delta MU_s \tag{12b}$$

It is straightforward to show from Eqs. (7) and (12) that

$$\frac{\left\langle \delta\Phi_{\Delta x}^{T=0} \right\rangle_{\sigma(PTV)}}{\left\langle \Phi^{T=0} \right\rangle_{\sigma(PTV)}} = \frac{\Delta x}{ALPO + 2 \cdot RFO} \tag{13}$$

*(iii)* $\mathrm{T} \neq 0, \; \mathrm{RFO} \neq 0$

Now let us include non-zero MLC transmission T. There is a simple algebraic relationship between primary fluence, $\Phi^{T=0}(x,y)$, and total fluence, $\Phi(x,y)$. The total fluence included fluence from MLC transmission. From Figure 3,

$$\begin{aligned} \Phi(x,y) &= \Phi^{T=0}(x,y) + T \cdot \left( MU_{total} - \Phi^{T=0}(x,y) \right) \\ &= (1-T) \cdot \Phi^{T=0}(x,y) + T \cdot MU_{total} \end{aligned} \tag{14}$$

Where $MU_{total}$ is the total MU required to deliver the dynamic MLC field, e.g., $MU_{total} = \sum_s \Delta MU_s$. And therefore using Eq. (12),

$$\langle \Phi \rangle_{\sigma(PTV)} = (1-T) \cdot \left\langle \Phi^{T=0} \right\rangle_{\sigma(PTV)} + T \cdot MU_{total} \tag{15a}$$

$$\langle \Phi_{\Delta x} \rangle_{\sigma(PTV)} = \langle \Phi \rangle_{\sigma(PTV)} + (1-T) \cdot \frac{w \cdot \Delta x}{\sigma(PTV)} \sum_{s,j=\text{openpair}} \Delta MU_s \qquad (15b)$$

Again it is straightforward to demonstrate from Eqs. (12) and (15) that

$$\frac{\langle \delta\Phi_{\Delta x} \rangle_{\sigma(PTV)}}{\langle \Phi \rangle_{\sigma(PTV)}} = \frac{\Delta x}{ALPO + 2 \cdot RFO + \varepsilon} \qquad (16)$$

in which $\varepsilon$ can be expressed as

$$\varepsilon \equiv \frac{T}{1-T} \frac{\sigma(PTV)}{w} \frac{MU_{total}}{\sum_{s,j=\text{open pairs}} \Delta MU_s} \qquad (17)$$

Notice that even though in the derivation we assumed step and shoot dynamic MLC, the final results (Eqs. (16) and (17)) are general and valid for sliding window dynamic MLC. $\varepsilon$ is generally of the order of 1 mm. The magnitude of $\varepsilon$ can be estimated as follows. Notice that $\sum_s \Delta MU_s = MU_{total}$. Therefore,

$$\frac{MU_{total}}{\sum_{s,j=\text{open pairs}} \Delta MU_s} = \frac{\sum_s \Delta MU_s}{\sum_{s,j=\text{open pairs}} \Delta MU_s} = \frac{\sum_s \Delta MU_s}{\sum_s (\text{number of open leaf pairs in subfield}) MU_s} \qquad (18)$$

$$= \frac{1}{\text{average number of open leaf pairs for DMLC field}}$$

For example, if $\sigma(PTV) = 10 \times 10\ cm^2$, $w = 1\ cm$, T = 2%, and approximating average number of open leaf pairs to irradiate a $10 \times 10 cm^2$ field to be 10, we get $\varepsilon$ = 2 mm. Similarly, for $\sigma(PTV) = 5 \times 5\ cm^2$, and approximating the average number of open leaf pairs to irradiate $5 \times 5\ cm^2$ to be 5, we get $\varepsilon$ = 1 mm.

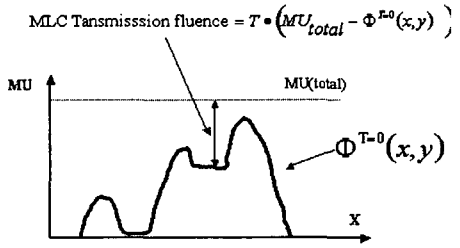


Figure 3. Fluence contribution from MLC transmission.

## 2.5. Numerical verification of the analytic relationship $\frac{\langle \delta\Phi_{\Delta x} \rangle_{\sigma(PTV)}}{\langle \Phi \rangle_{\sigma(PTV)}} = \frac{\Delta x}{ALPO + 2 \cdot RFO + \varepsilon}$

The analytic relationship (Eq. 16) between a fractional fluence error from a systematic gap error of $\Delta x$ and ALPO is elegantly simple. We tested the validity of this relationship with a numerical simulation.

At Massachusetts General Hospital, the HELIOS sliding window IMRT system was commissioned for 6MV Varian CL2100 with rounded end 26 pair MLC (Varian Oncology System, Palo Alto, CA). Leaf width is 1 cm at 100 SAD projection. We used RFO = 0.75 mm and $T = 1.5\%$ for the MLC transmission. Helios IMRT plans were generated for sites, i.e., head & neck, lung, and abdomen. Each IMRT plan had 5 to 8 portal fields. For each of the portal field, we calculated $\frac{\langle \delta\Phi_{\Delta x} \rangle_{\sigma(PTV)}}{\langle \Phi \rangle_{\sigma(PTV)}}$ both analytically, Eq. (16), and numerically, Eqs. (4) –(7), and the results were compared. We used the numerical simulation results as benchmark values.

### 2.6. Dosimetric Study

According to Eq. (16), average fluence error incident on skin from a systematic gap error of $\Delta x$ is $\Delta x / (ALPO + 2 \cdot RFO + \varepsilon)$. This implies that an average dose error to PTV per IMRT field from a gap error of $\Delta x$ should also be approximately $\Delta x / (ALPO + 2 \cdot RFO + \varepsilon)$. A direct verification of this would require an ionization chamber with an active volume of PTV for proper dose averaging. Because of this difficulty, we verified this statement for a very specific type of dynamic MLC field. A sweeping window dynamic MLC file (fixed leaf-to-leaf separation) was made to deliver a "uniform" 14x25cm$^2$ fluence (Fig. 4). In order to simulate a systematic MLC calibration error of $\Delta x = 1\ mm$, a second sweeping window dynamic MLC file was created with each leaf position offset by 0.5 mm from the original dynamic MLC file (Eq. 5). A 0.1cc active volume Farmer chamber was placed at d = 10 cm SAD, irradiated with the original and the offset dynamic MLC files, and the electrometer readings were recorder. This experiment was repeated for sweeping window dynamic MLC with different fixed leaf-to-leaf openings ranging from 0.5 cm to 5 cm.

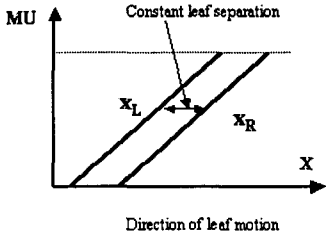


Figure 4. Leaf trajectories for a sweeping window dynamic MLC delivery with a constant leaf- to-leaf separation, e.g., $(x_R - x_L) = \text{constant}$.

## 3. RESULTS

### 3.1. Results for comparing analytic and numerical calculation of $\frac{\langle \delta\Phi_{\Delta x} \rangle_{\sigma(PTV)}}{\langle \Phi \rangle_{\sigma(PTV)}}$

Tables I (a, b, c) show three IMRT plans and the corresponding ALPO values, as well as analytically and numerically calculated values of $\frac{\langle \delta\Phi_{\Delta x} \rangle_{\sigma(PTV)}}{\langle \Phi \rangle_{\sigma(PTV)}}$. The agreement between the analytic and numerical calculation is clear. If dosimetry is to be accurate to within 5%, than all of these IMRT plans are too sensitive to a systematic MLC gap error $\Delta x$ of 1 mm and the plans should be rejected. At Massachusetts General Hospital, our estimate for the systematic MLC gap accuracy is approximately $\Delta x = 0.5\ mm$. Therefore, all the predicted fluence error of Tables I(a, b ,c) were reduced by a factor of 2.

Table 1 (a), b), (c) Three IMRT plans for various sites showing ALPO for each field. Columns 3 and 4 show comparisons of analytic and numerical calculations of average fluence error from a systematic MLC gap error of $\Delta x$.

(a) Head & Neck 6MV, T = 1.5%, RFO = 0.75mm Δx = 1mm

| Field # | $ALPO+2 \cdot RFO+\varepsilon$ | $\Delta x/(ALPO+2 \cdot RFO+\varepsilon)$ | Numerical Calculation of $\{\delta\Phi_{\Delta x}\}_{\sigma(PTV)}/\{\Phi\}_{\sigma(PTV)}$ |
|---|---|---|---|
| 1 | 1.31 | 7.6% | 7.0% |
| 2 | 1.32 | 7.5% | 6.4% |
| 3 | 1.41 | 7.1% | 7.5% |
| 4 | 1.35 | 7.4% | 6.3% |
| 5 | 1.38 | 7.2% | 8.3% |
| 6 | 1.35 | 7.4% | 8.2% |
| 7 | 1.31 | 7.6% | 7.8% |
| 8 | 1.32 | 7.6% | 8.3% |

(b) Lung 6MV, T = 1.5%, RFO = 0.75mm Δx = 1mm

| Field # | *ALPO+2·RFO+ε* | Δx/(*ALPO+2·RFO+ε*) | Numerical Calculation of $\{\delta\Phi_{\Delta x}\}_{\sigma(PTV)}/\{\Phi\}_{\sigma(PTV)}$ |
|---|---|---|---|
| 1 | 1.72 | 5.8% | 6.8% |
| 2 | 2.01 | 5.0% | 4.1% |
| 3 | 2.37 | 4.2% | 5.1% |
| 4 | 1.24 | 8.1% | 7.7% |
| 5 | 1.43 | 7.0% | 6.3% |

(c) Abdomen 6MV, T = 1.5%, RFO = 0.75mm Δx = 1mm

| Field # | *ALPO+2·RFO+ε* | Δx/(*ALPO+2·RFO+ε*) | Numerical Calculation of $\{\delta\Phi_{\Delta x}\}_{\sigma(PTV)}/\{\Phi\}_{\sigma(PTV)}$ |
|---|---|---|---|
| 1 | 1.20 | 8.3% | 8.3% |
| 2 | 1.14 | 8.8% | 8.7% |
| 3 | 1.16 | 8.6% | 8.7% |
| 4 | 1.35 | 7.4% | 7.4% |
| 5 | 1.70 | 5.9% | 6.1% |
| 6 | 1.07 | 9.3% | 9.1% |
| 7 | 1.34 | 7.5% | 7.4% |
| 8 | 1.28 | 7.8% | 7.7% |

### 3.2. Results for dosimetric studies

Table II, summarizes the dosimetry study for sweeping window of various sizes. Because dose for a sweeping window test is uniform across the field, one-point ionization chamber measurement was sufficient and there was no measurement due to a possible miss-positioning of the detector. For these sweeping window dynamic MLC delivery, $\Delta x/(ALPO+2\cdot RFO+\varepsilon)$ is shown to be an estimator of both average fluence and dose errors.

Table 2. Chamber measurement demonstrating, for sweeping window dynamic MLC delivery, that $\Delta x/(ALPO+2\cdot RFO+\varepsilon)$ is an average dose error. Sweeping window tests 1-4 were performed for various ALPO values.

| Field # | *ALPO+2·RFO+ε* | Δx/(*ALPO+2·RFO+ε*) | Numerical Calculation of $\{\delta\Phi_{\Delta x}\}_{\sigma(PTV)}/\{\Phi\}_{\sigma(PTV)}$ | ΔD/D chamber |
|---|---|---|---|---|
| 1 | 5.4 | 1.9% | 1.1% | 0.9% |
| 2 | 3.4 | 2.8% | 2.3% | 2.2% |
| 3 | 2.0 | 4.7% | 4.4% | 4.0% |
| 4 | 0.5 | 18.9% | 21.9% | 22.9% |

## 4. DISCUSSION AND CONCLUSION

We introduce a concept of Average Leaf Pair Opening (ALPO). We derived an analytic relationship between an average fluence error and a systematic MLC gap error of $\Delta x$, e.g., $\Delta x/(ALPO+2\cdot RFO+\varepsilon)$. This analytic result was verified with numerical simulations. We also demonstrated for a sweeping dynamic MLC delivery that not only fluence but also average dose error to PTV from a systematic gap error of $\Delta x$ is also approximately $\Delta x/(ALPO+2\cdot RFO+\varepsilon)$. As an example, for dosimetry to be accurate within 5% for a dynamic MLC file with $ALPO+2\cdot RFO=1\ cm$, the MLC gap error $(\Delta x)$ must be smaller than 0.5 mm. In the future work with phantom measurements, we will further investigate the relationship between the average fluence error, Eq. (16), and the average dose error to the PTV.

As mentioned in the introduction, several authors have quoted different values of RFO for 6 MV Varian rounded end MLC, e.g., 0.2 mm[11], 0.75 mm[12], 0.95 mm[8], 0.6 mm[14]. With the concept of ALPO, we can now readily address the question of dosimetric effect of using an inaccurate RFO value into an IMRT treatment planning system. At

Massachusetts General Hospital (MGH), we commissioned the Helios IMRT system with RFO = 0.75 mm, and the dosimetry along the central axis in water equivalent solid phantom with ionization chambers was within 5%. With a feeler gauge, we estimated an upper bound on CMO to be 0.5mm. At MGH, we only accept dynamic MLC plans with $ALPO + 2 \cdot RFO \geq 1\ cm$. Consider a hypothetical situation of switching to RFO = 0.95 mm without changing CMO. Then all MLC gaps change will change by $\Delta x = 2\Delta\mathrm{RFO} = 2 \cdot (0.95 - 0.75)\ \mathrm{mm} = 0.4\ \mathrm{mm}$. Therefore the dosimetry will change by at most by 4% for $ALPO + 2 \cdot RFO \geq 1\ cm$. On the other extreme, switching to RFO = 0.2 mm will change all gaps by $\Delta x = 2 \cdot (0.75 - 0.2)\ \mathrm{mm} = 1.1\ \mathrm{mm}$, and dosimetry can change by as much by 11% for $ALPO + 2 \cdot RFO \geq 1\ cm$.

We can find two reasons why different departments were able to commission IMRT for 6MV and Varian MLC using different values of RFO without noticing serious dosimetric errors. A) Because $\Delta x = \mathrm{CMO} + 2\Delta\mathrm{RFO}$, it is possible to have several combinations of CMO and $\Delta RFO$ resulting in the same small $\Delta x$. B) Fractional fluence error is proportional to $\Delta x / ALPO$. If an IMRT treatment planning system consistently produce plans with large ALPO values for dynamic MLC deliveries, then even with wrong combination of CMO and RFO values, dose error would not have been unnoticeable. These sample calculations show the utility of ALPO concept.

We propose to use parameters like ALPO to identify and reject a dynamic MLC delivery that is highly sensitive to a systematic MLC gap error. Should one wishes to decrease the sensitivity of MLC delivery to gap errors, we suggest: (a) reduce CMO and improve determination of RFO in order to decrease Δx, and (b) enlarge ALPO. However, the latter can only be done by the manufacturer of an IMRT system.

## REFERENCES


1. S. Spirou, C. Chui, "Generation of arbitrary intensity profiles by dynamic jaws or multileaf collimator," Med. Phys. **21**, 1031-1041 (1994).
2. L. Ma, A. L. Boyer, L. Xing, C. M. Ma, "An optimized leaf sequencing algorithm for beam intensity modulation using dynamic multileaf collimator," Phys. Med. Biol. **43**, 1629-1643 (1998).
3. J. Stein, T. Bortfeld, B. Dorschel, W. Schlegel, "Dynamic X-Ray Compensation for Conformal Radiotherapy by Means of Multileaf Collimation," Radiother. Oncol. **32**, 163-173 (1994).
4. A. Brahme, "Optimization of stationary and moving beam radiation therapy technique," Radiother. Oncol. **12**, 129-140 (1988).
5. P. Kallman, B. Lind, A. Eklof, et. al., "Shaping of arbitrary dose distribution by dynamic multileaf collimator," Phys. Med. Biol. **33**, 1291-1300 (1988).
6. D. J. Convery, M. E. Rosenbloom, "The generation of intensity modulated fields for conformal radiotherapy by dynamic collimation," Phys. Med. Biol. **37**, 1359-1374 (1992).
7. C. S. Chui, S. Spirou, T. LoSasso, "Testing of dynamic multileaf collimation," Med. Phys. **23**, 635-641 (1996).
8. T. LoSasso, C. S. Chui, C. C. Ling, "Physical and dosimetric aspects of a multileaf collimation system used in the dynamic mode for implementing intensity modulated radiotherapy," Med. Phys. **25**, 1919-1927 (1998).
9. C. D. Mubata, P. Childs, A. M. Bidmead, "A quality assurance procedure for the Varian Multi-leaf Collimator," Phys. Med. Biol. **42**, 423-431 (1997).
10. E. E. Klein, W. B. Harms, D. A. Low, et al. " Clinical Implementation of a Commercial Multileaf Collimator: Dosimetry, Networking, Simulations, and Quality Assurance," Int. J. Rad. Onc. Biol. Phys. **33**, 1195-1208 (1995).
11. A. L. Boyer, S. Li, "Geometrical analysis of light-field position of a multileaf collimator with curved ends," Med. Phys. **24**, 757-762 (1997).
12. L. Xing, B. Bruce, A. Beavis, A. Kapur, J. Li, Y. Chen, A. Boyer, "Minimizing the Dosimetric Effect of the Rounded MLC leaf ends," Med. Phys. **26**, 1087 (1998).
13. L. S. Johnson, F. T. Kuchnir, C.S. Reft, J. H. Kung, "Clinical Implementation of Intensity Modulated Radiotherapy Using a Dynamic Multi-leaf Collimator", Med. Phys. **26**, 1086 (1999).
14. M. R. Arnfield, J. V. Siebers, J. O. Kim, Q. Wu, P. J. Keall, R. Mohan, "A Method of Determining Multileaf Collimator Transmission and Scatter for Dynamic Intensity Modulated Radiotherapy," Med. Phys. **27**, 2231-2241 (2000).
15. J. H. Kung, G. T. Y. Chen, "IMRT Dose delivery error from Radiation Field Offset Inaccuracy," Med. Phys. **27**, 1617-1622 (2000).
16. J.H. Kung, G. T. Y. Chen, F. T. Kuchnir, "A Monitor Unit Verification Calculation in IMRT as a Dosimetry QA," Med. Phys. **27**, 2226-2240 (2000).